Structures 29 (2021) 1507–1521

Contents lists available at ScienceDirect

Structures

journal homepage: www.elsevier.com/locate/structures

Finite element modelling of castellated steel beams under lateral-distortional buckling mode

Mahmoud Hosseinpour, Yasser Sharifi *

Department of Civil Engineering, Vali-e-Asr University of Rafsanjan, Rafsanjan, Iran

ARTICLE INFO

Keywords:
Castellated steel beam
Lateral-distortional buckling
Finite element modelling
Numerical study
Structural design code

ABSTRACT

This paper examined the effects of web distortion on the buckling behavior of castellated steel beams. To this purpose, a series of nonlinear finite element (FE) models was constructed and well verified against an experimental work on the distortional buckling of castellated beams; both material nonlinearities and initial geometric imperfections were carefully applied to the models. Next, an extensive parametric study was performed using the finite element models to investigate the effects of beam length, steel grade and cross-section dimensions on the ultimate buckling load and buckling modes of castellated steel beams. The results showed that the use of low grade steel and thick flanges makes an economical design in the castellated steel beams. Moreover, it is concluded that lateral-distortional buckling (LDB) mode is more common in the castellated beams with intermediated overall slenderness, thick flanges and slender web. Finally, the ultimate loads obtained from finite element analysis (FEA) were compared with the results predicted by AS4100, EC3 and AISC codes. It was concluded that all three Specifications provide unsafe estimates for most specimens in this study.

1. Introduction

Castellated beams are prepared by flame cutting the standard hot-rolled beams along their centerline and then welding the two halves obtained by cutting. Since, the height of castellated beams increases through this process, the performance of these beams against bending is improved, which leads to an economic design. Moreover, other benefits of these beams comprise optimum weight, larger section modulus, and ease of service through the web openings. On the other hand, castellated beams are liable to different failure modes including shear failure, flexural failure, lateral-torsional buckling, local buckling, rupture of welded joints and web post-buckling. The occurrence of each of these failure modes depends on the locations of lateral supports, web slenderness, flange slenderness, welding quality, geometry and dimensions of web openings, and also the loading type [1–5].

The buckling phenomenon is one of the most important issues in steel members due to their slender systems. In general, I-shaped beams under load inside the plane, are prone to local and lateral torsional buckling (LTB), depending on the web slenderness, flange slenderness as well as overall slenderness of the beam. On the other hand, due to the fact that castellated beams have a deeper cross-section than the sections from which they are made, they are more prone to LTB mode; this mode usually occurs when the compression flange of the beam is not supported laterally. In LTB mode, the beam cross-section twists as a rigid body while no distortion occurs on the web; on the contrary, in local buckling mode, web and/or flange buckle(s) locally over a short distance and without global rotation of the beam [6–10]. A beam under lateral load that is bent about its major axis can buckle sideways if its compression flange has insufficient stiffness in the lateral direction. At a critical load, the plate-stiffener combination model can become unstable because the compression flange may twist sideways. This phenomenon is sometimes termed lateral-torsional buckling (or tripping), which is generally considered to be one of the many types of behavior that may lead to the ultimate limit state (ULS) of the plate-stiffener combination model [11].

In addition to the two above-mentioned modes, in the I-shaped beams with intermediate length, slender web and stocky flanges, overall lateral buckling may be accompanied with web distortion, creating a new type of buckling mode, called lateral-distortional buckling (LDB). This mode is described with simultaneous occurrence of lateral translation, twisting and web distortion; and usually occurs in the intermediate-length beams with slender web and thick flanges [12]. It should be mentioned that generally distortional buckling has been recognized in two modes including: “lateral-distortional buckling” (LDB) and “restrained distortional buckling” (RDB) (See Fig. 1);

* Corresponding author.
E-mail addresses: y.sharifi@vru.ac.ir, yasser_sharifi@yahoo.com (Y. Sharifi).

https://doi.org/10.1016/j.istruc.2020.12.038
Received 9 October 2020; Received in revised form 7 December 2020; Accepted 20 December 2020
Available online 1 January 2021
2352-0124/© 2020 Institution of Structural Engineers. Published by Elsevier Ltd. All rights reserved.

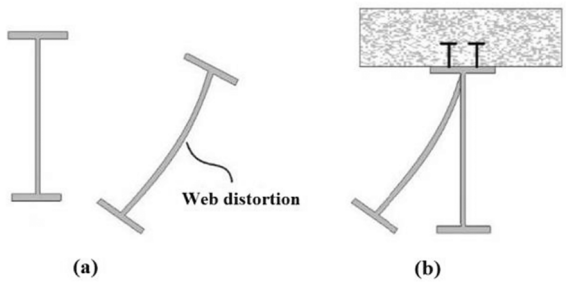

Fig. 1. Distortional buckling: (a) LDB (b) RDB.

furthermore, RDB, may occur in any situation where the tension flange is restrained against lateral translation and twisting, e.g. in the negative moment regions of composite beams or in the half-through girder bridges [13–15].

To date, extensive studies have been conducted to investigate the distortional buckling behavior of doubly symmetric I-beams in which Bradford has made a significant contribution [16–22]. Bradford and Wee [20] conducted a series of eight beams supported on seats, because only the top compressive flange was restrained with the stiffness of web, the dominant buckling mode was observed distortional. Moreover, finite element method was used to analyze the tests, and also the codes' predictions were compared with the results of tests and theoretical solutions.

Vrcelj and Bradford [21] examined the effects of combined uniform axial force and moment gradient on the elastic buckling load of beam-columns with simply supports. They used an energy method of analysis and developed a simple method to predict the elastic RDB load of beam-columns under combined uniform axial force and moment gradient. The results showed that a linear interaction equation is appropriate for predicting the out-of-plane buckling strength of beam-columns.

The accuracy of AISC code for determination of the elastic distortional buckling strength of I-section members, was investigated by Zirakian [22]. A comparison was made between the AISC predictions and the results of finite strip analysis and theoretical solutions; it was found that AISC code provided conservative predictions for distortional buckling of I-shaped members with slender web.

Another study on the distortional buckling behavior of beams was performed by Zirakian and Showkati [23]. They studied the behavior of distortional buckling of castellated steel beams through an experimental work. Due to the fact that so far no experimental work has been done on the distortional buckling of castellated steel beams, therefore, the mentioned literature provides useful information comprising buckling modes, failure loads and load-lateral deflection curves, which can be used for development of numerical models in order to investigate the buckling behavior of castellated steel beams. The details of this work are described in Section 2.

Since, to date no numerical study has been found, highlighting the LDB behavior of castellated beams, the current paper presents an extensive numerical study based on the finite element method to examine the LDB behavior of castellated steel beams. In general, the finite element models obtain a better understanding of the behavior of structural elements. Therefore, the main purpose of this study is employment of the finite element analysis (FEA) to investigate the inelastic lateral distortional behavior of castellated steel beams subjected to a concentrated load at mid-span. To this purpose, finite element analyzes were accomplished using finite element program ABAQUS [24], which considered both initial geometric imperfections and material nonlinearities. Moreover, the parametric study was established using FEA results to specify the effects of beam length, steel strength and cross-section dimensions on the failure loads and buckling modes of castellated steel beams.

2. Summary of experimental study

In order to validate the numerical study accomplished in this paper, it is necessary to confirm the numerical results against the experimental results. For this purpose, an experimental study on the buckling of castellated beams was used, which is summarized in this section. Zirakian and Showkati [23] conducted six full-scale tests on the simply supported castellated steel beams with a central concentrated load. The dimensions and material properties of the castellated beams are given in Table 3, while the corresponding notations are illustrated in Fig. 2. The castellated beams were labeled in such a way that their nominal depth and length could be identified, each specimen label begins with the letter C, followed by the nominal depth and followed by the length (e.g. 'C210-3600' indicated the castellated beam with a nominal depth of 210 mm and a length of 3600 mm).

The specimens were designed such as the lateral displacements at mid-span and at the distances of 165 mm from the end supports were restrained using lateral bracing. The load was then applied to specimens using a 608 kN hydraulic jack until failure occurred. During testing process, lateral displacements and web strains were recorded continuously at the middle and a quarter of span. Since lateral displacements of the compression flange at mid-span as well as near both end supports were prevented (See Fig. 3), therefore, the beam cross-section at mid-span and quarter-span were exposed to RDB and LDB, respectively. The results of the tests are given in details in Section 3.1 to be used as a reference in the validation of numerical models.

3. Finite element models

The main objective of the current paper is to study the LDB behavior of castellated steel beams using finite element method, consequently, the finite element (FE) program ABAQUS, was used to model castellated steel beams subjected to lateral-distortional buckling. Buckling analysis needs two different types of analysis, the first one is known as Eigenvalue analysis which predicts both buckling load and buckling mode. The lowest buckling mode estimated by Eigenvalue analysis is then used for the next analysis which is a load–displacement nonlinearity analysis, known as RIKS method in ABAQUS library [24]; RIKS method is usually used to obtain nonlinear and unstable collapse of a structure. Therefore, in this study a full Newton-Raphson technique together with an Arc Length Control Iterative and an automatic incrimination strategy was used through the RIKS method to solve the nonlinear equations.

In ABAQUS library, the three-node and four-node doubly curved shell elements with reduced integration (the elements S3R and S4R, respectively), are capable for simulation of the complex buckling behavior of beams; hence, these elements were used to model the castellated steel beam in this study. The S3R and S4R elements have six degrees of freedom per node and present a precise solution for most problems; furthermore, they are appropriate for large strain analysis [25]; and considering that the lateral buckling of beams are very sensitive to large strains, the S3R and S4R elements were suitable for this study.

The boundary conditions of FE models were considered identical to

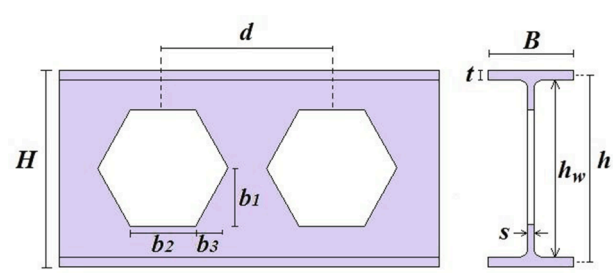

Fig. 2. Beam and castellation geometries.

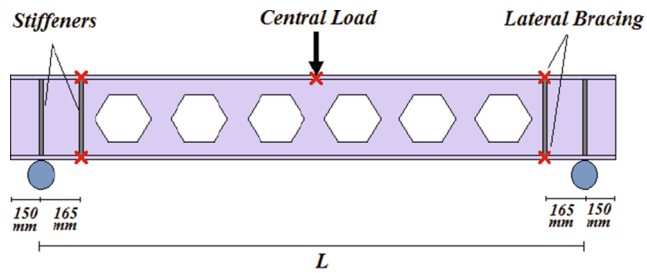

Fig. 3. Test arrangement.

the experimental tests conducted in Ref. [23]. As depicted in Fig. 4, lateral displacement of the top compression flange was restrained at the middle of span while lateral displacement of both flanges was restrained at the distances of 165 mm from the end supports. Moreover, similar to the tests, the static concentrated load was applied in incremental steps to the middle of span.

To model the behavior of materials in FE specimens, the stress–strain curve of structural steel, based on EC3 [26], was adopted and material nonlinearities were applied to the FE models using PLASTIC option provided by ABAQUS program; this option allows the nonlinear stress–strain curve to be used for modeling. The typical values of Poisson's ratio and Young's modulus were set at 0.3 and 200,000 MPa, respectively. Moreover, since lateral buckling includes large strains, the engineering stress and strain were changed to true stress (σ_{true}) and logarithmic plastic true strain (ε^{pl}_{true}), using Eqs. (1) and (2) [24], respectively, and then true stress–strain curve was applied into the FE models.

$$\sigma_{true} = \sigma(1+\varepsilon) \tag{1}$$

$$\varepsilon^{pl}_{true} = In(1+\varepsilon) - \sigma_{true}/E \tag{2}$$

where σ and ε show the nominal stress and nominal strain, respectively; and E shows the modulus of elasticity.

The structural steel elements are exposed to initial geometric imperfections due to their production procedure. Generally, the imperfections in the design stage are unidentified due to estimation of amplitude and pattern, they are usually taken as random quantities which can be attained using stochastic methods. In practice, a more practical deterministic method is used to apply the initial geometric imperfections, in such a way that the displacements of the first buckling mode shape are used as the initially imperfect shape of the member. Accordingly, knowledge of the maximum displacements of the first (fundamental) buckling mode, based on the eigenvalue analysis, is generally adequate to define the most effective imperfections [27–29].

On the other hand, because the buckling modes estimated by Eigenvalue analysis are generalized to 1.0, the buckling modes are scaled by a value of geometric imperfection, and consequently the lowest scaled buckling mode is placed into the RIKS (load–displacement) analysis of the member. In this paper, the geometric imperfection were applied to the models by considering a half-since wave lateral imperfection with amplitude $L_b/1000$, where L_b is the length between the points of effective bracing. In general, the magnitude of $L_b/1000$ has been recognized as an average value for test measurements in previous researches [12–15,30–32], this specific value for initial imperfection is also stated in AS4100 as a fabrication tolerance for flexural elements.

Furthermore, it is worth mentioning that based on the previous literatures, the residual stresses due to the manufacturing process had small influences on the buckling behavior of different structural elements and researchers had often ignored this in their researches [12–15,32–36]; as a result, residual stresses are not comprised in this study, however, it is relevant in this type of analysis.

3.1. Finite element model verification

The developed FE models were verified against the tests' results conducted in Ref. [23], which were previously described in Section 2; as mentioned before, the literature has provided useful information comprising buckling modes, failure loads and load-lateral deflection curves, which can be used for the verification of numerical models in this study. Therefore, six castellated beams with the dimensions and yield stresses given in Table 1, were modeled using finite element software ABAQUS, and their results were obtained. Table 2 reveals the comparison between the results of FE models and experimental work. As it is clear form Table 2, except for specimens C180-5200 and C210-4400 with unacceptable results in experimental work, there was a good match between the results of FEA and experimental work in other specimens, such that the average error between the results of numerical and experimental studies was less than one percent. Moreover, the dominant mode in all numerical specimens was LDB mode, which was exactly in accordance with the experimental results.

The load-lateral displacement curves of specimen C180-3600, were other information provided in the experimental work. The curves were plotted for the top, middle and bottom points of the web at quarter-span; as a result, the similar points were considered in the FE model of specimen C180-3600, and the load-lateral displacement curves were plotted for them. Fig. 5 shows the comparison between numerical and experimental curves; as can be seen from the figure, there is a good agreement between the curves related to numerical and experimental studies. For experimental specimen, the maximum lateral displacement at failure was 5.7, 2.8 and −1 mm related to the top, middle and bottom points of the web, respectively, while these values for FE model were obtained 6.4, 3.6 and −0.9 mm. This should be noted that, the negative and positive signs denote lateral displacement in back and front of the web, respectively.

3.2. Parametric study

Based on the verified FE models, 480 castellated beams were modeled by finite element program ABAQUS, to examine the distortional buckling behavior of castellated steel beams. The modeled

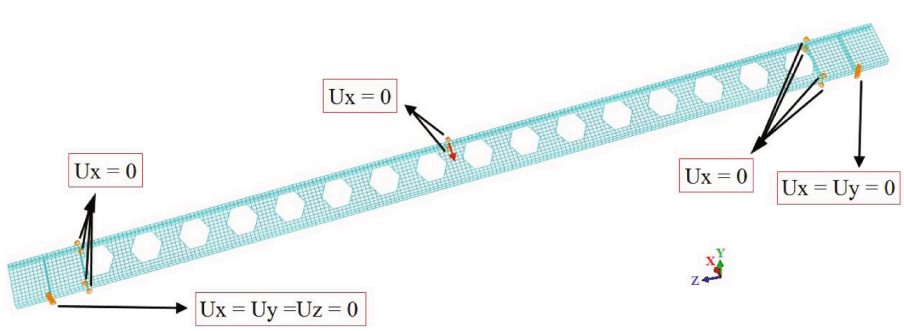

Fig. 4. Boundary conditions in finite element models.

Table 1
Dimensions and material properties of castellated steel beams reported in Ref. [23].

Specimen	Dimension (mm)									Yield Stress (MPa)	
	b_3	b_2	b_1	d	L	s	t	B	H	Web	Flange
C180-3600	30	60	60	180	3600	4.4	6.3	64	176.3	234	279
C180-4400	30	60	60	180	4400	4.4	6.3	64	176.3	234	279
C180-5200	30	60	60	180	5200	4.4	6.3	64	176.7	234	279
C210-3600	35	70	70	210	3600	4.7	6.9	73	206.5	332	280
C210-4400	35	70	70	210	4400	4.7	6.9	73	210.3	332	280
C210-5200	35	70	70	210	5200	4.7	6.9	73	211.7	332	280

Table 2
Comparison between results of tests and finite element models.

Specimen	Experimental		Finite Element		Err (%)
	Failure Mode	Failure Load (kN)	Failure Mode	Failure Load (kN)	
C180-3600	LDB	21.58	LDB	21.9	1.48
C180-4400	LDB	15.63	LDB	15.86	1.47
C180-5200	LDB	25.92[a]	LDB	14.38	–
C210-3600	LDB	37.22	LDB	37.01	0.78
C210-4400	LDB	39.94[b]	LDB	28.63	–
C210-5200	LDB	24.90	LDB	24.85	0.20
					Mean = 0.98

[a] Due to the influence of initial geometric imperfections and interaction between the buckling behaviors of the two adjacent spans, failure of the beam has occurred at a higher load than the expected amount [23].
[b] Because of some frictional restraint at the loading point, which was observed during the test, the test strength is high compared to those for the other C210 beams [23].

specimens were divided into six groups named G1 to G6, in such a way that each group included 80 specimens by identical length (L), center to center distance of flanges (h), flange width (B), distance between castellations (d) and castellation dimensions (b_1, b_2, and b_3), but with different flange thickness (t), web thickness (s) and steel yield stress (F_y). It should be noted that for each group, parameters L, h, B, d, b_1, b_2 and b_3 were considered similar to one of the castellated beams tested in the experimental study [23]. In the present parametric study, thick flanges and slender web were used to increase the probability of LDB mode occurring in the specimens; therefore, four web thicknesses of 3, 4, 5 and 6 mm and four flange thicknesses of 6, 8, 10 and 12 mm were used to model the specimens. Moreover, to examine the effects of steel grade on the bucking behavior of castellated steel beams, five yield stresses including 275, 345, 460, 550 and 690 MPa were considered in the modeling. Table 3 shows the considered dimensions and yield stresses of specimens in this study, unlike experimental specimens, the yield stresses of the flanges and web of each FE model was considered the same. Consequently, the modeled castellated beams were analyzed and the main results including failure loads and buckling modes were obtained, which are discussed in the next section.

4. Results and discussions

4.1. Buckling modes

By examining the buckling modes of all specimens, it was concluded that, as expected, most specimens were failed in the LDB mode. From 480 modeled castellated beams, the buckling mode of 436 specimens were LDB, while the buckling mode of 20 and 24 beams were LTB and web distortion (WD), respectively. Figs. 6 and 7 show the shapes of different modes which were obtained from the results of finite element analyzes.

As it is clear from Fig. 6, in the WD mode, the web of castellated beams buckle locally over a short distance, from 24 specimens with WD mode, two specimens were related to group G1, nineteen specimens were related to G4 and three specimens were related to G5; therefore, it can be seen that as the beam length decreases and the web height increases, the probability of occurrence of WD mode increases. Moreover, most specimens by WD mode, had a web thickness of 3 mm, flange thicknesses of 10 and 12 mm, and yield stresses of 275 and 345 MPa; consequently, by decreasing the web thickness and yield stress and also

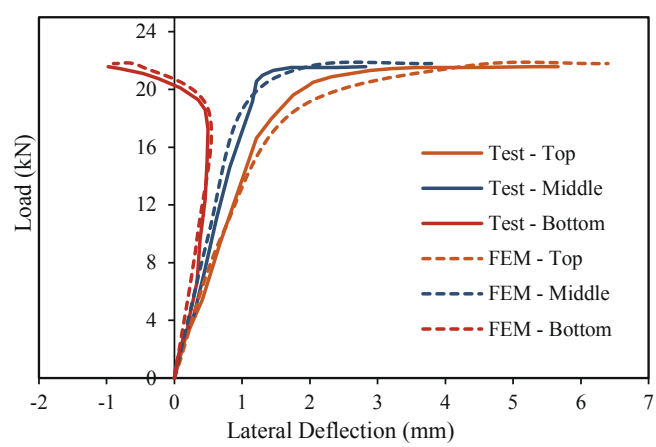

Fig. 5. Comparison between load-lateral displacement curves related to specimen C180-3600.

Table 3
Dimensions and material properties of specimens.

Group	Dimensions (mm)									F_y (MPa)
	L	h	B	d	b1	b2	b3	s	t	
G1 (S1-S80)	3600	170	64	180	60	60	30	3,4,5,6	6,8,10,12	275,345,460,550,690
G2 (S81-S160)	4400	170	64	180	60	60	30	3,4,5,6	6,8,10,12	275,345,460,550,690
G3 (S161-S240)	5200	170.4	64	180	60	60	30	3,4,5,6	6,8,10,12	275,345,460,550,690
G4 (S241-S320)	3600	199.6	73	210	70	70	35	3,4,5,6	6,8,10,12	275,345,460,550,690
G5 (S321-S400)	4400	203.4	73	210	70	70	35	3,4,5,6	6,8,10,12	275,345,460,550,690
G6 (S401-S480)	5200	204.8	73	210	70	70	35	3,4,5,6	6,8,10,12	275,345,460,550,690

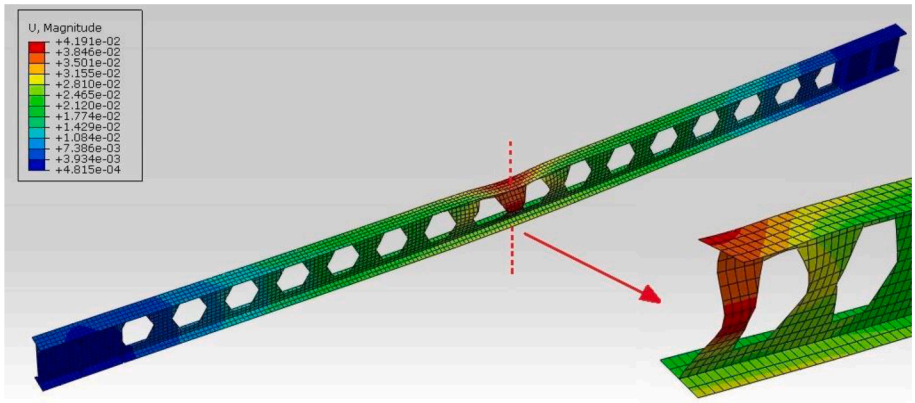

Fig. 6. Typical shape for WD buckling mode.

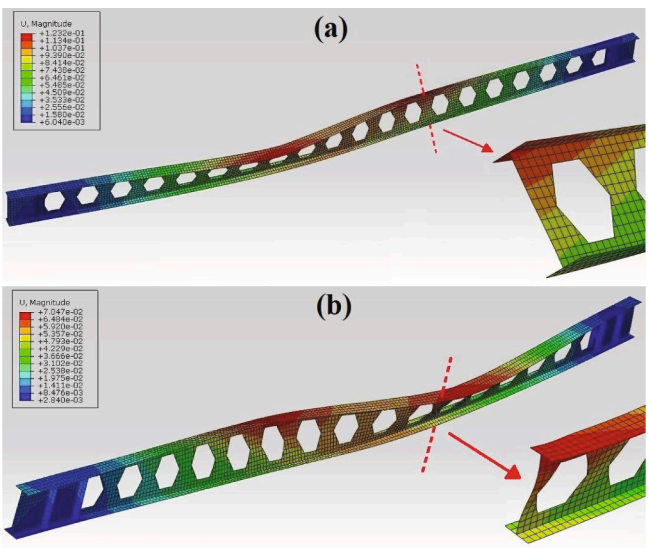

Fig. 7. Typical shapes for buckling modes: (a) LTB (b) LDB.

by increasing the flange thickness, WD dominates the failure mode.

Fig. 7 shows the mode shapes of LTB and LDB, the general shape of the two modes is similar to each other, except that in LTB mode no distortion is observed in the web and cross-section of beam twists as a rigid body, while in LDB mode, the overall lateral buckling is accompanied by web distortion, as it is clear form Fig. 7(b). Except for specimens with WD mode, for other specimens, the presence of web distortion was investigated, by examining the lateral displacement at different points of web height; out of 156 specimens, the buckling mode of 20 specimens was LTB, and no web distortion was found in them. Of these 20 specimens, five specimens were found in group G1, five specimens in group G2, six specimens in group G3 and four specimens in group G6; then by increasing the beam length and by decreasing the web height, the probability of occurrence of LTB mode increases. Moreover, Out of 20 specimens by LTB mode, 19 specimens had a web thickness and a flange thickness of 6 mm, which means that as the web thickness increases and the flange thickness decreases, the probability of LTB mode increases. Further, it was concluded that LTB mode is more common in the specimens with higher grade steel.

As mentioned before, the web and flange thicknesses as well as the lateral unbraced length of castellated beams exerted the greatest effect on changing the buckling mode, therefore, two parameters λ and αwere considered, such that λ represents the non-dimensional overall slenderness ratio which is equal to the ratio of unbraced length to minor-axis radius of gyration $\left(\frac{L_b}{r_y}\right)$, and α represents the ratio of flange slenderness to web slenderness $\left(\alpha = \frac{\lambda_f}{\lambda_w} = \frac{B/2t}{h_w/s}\right)$. The range of theses parameters for different buckling modes were compared in Table 4; as it is clear from the table, a similar trend can be observed for all groups, so that intermediate values of λ and α, can lead to LDB mode. Moreover, for castellated beams with lower amounts of λ and α, local bucking in the web (WD) dominates the failure mode, while LTB mode is also predominant for beams with higher values of λ and α.

4.2. Failure loads

In order to investigating the effects of variable parameters considered in this study on the failure loads of castellated steel beams, including web thickness, flange thickness and yield stress, for all specimens the collapse plastic load (P_{Pl}), corresponding to the major axis full plastic moment (M_{Pl}), was calculated as a reference respond, and then compared with the failure loads obtained from finite element analyzes (P_{FE}). The major axis full plastic moment can be calculated according to:

$$M_{Pl} = F_y . Z_x \tag{3}$$

where, F_y is the yield stress and Z_x is the plastic section modulus.

Fig. 8 shows the effects of web slenderness, flange slenderness and yield stress on the P_{FE}/P_{Pl} ratio for specimens of group G1; hence, the P_{FE}/P_{Pl} ratio was plotted against the flange slenderness ($B/2t$) for specimens with different steel grades. As it is illustrated in Fig. 8, for specimens by identical characteristics in group G1, as the flange slenderness decreases, the ratio of P_{FE}/P_{Pl} increases and therefore, more capacity of beam cross section (compared to the full plastic capacity) is consumed. A similar trend was observed for specimens in other groups G2-G5, in such a way that for the first to third groups, where the specimens had flange slenderness ratios of 5.3, 4.0, 3.2 and 2.7, in specimens with similar characteristics by reducing the flange slenderness from 5.3 to 2.7, the P_{FE}/P_{Pl} ratio increased between 0.08 and 0.25; moreover, for the forth to sixth groups, where the specimens had flange slenderness ratios of 6.1, 4.6, 3.7 and 3.0, in specimens with similar characteristics by reducing the flange slenderness from 6.1 to 3.0, the P_{FE}/P_{Pl} ratio increased between 0.07 and 0.23.

On the other hand, as it is clear form Fig. 8(a)–(d), for specimens with similar characteristics in group G1, by decreasing the yield stress, the ratio of P_{FE}/P_{Pl} increases, in such a way that as the yield stress decreased from 690 to 275 MPa, the P_{FE}/P_{Pl} ratio increased between 0.21 and 0.25, therefore, up to 25% more cross-section capacity was used compared to the full plastic capacity. By examining the second to sixth group, a similar trend was found for them; by reducing the yield stress from 690 to 275 MPa, the ratios of P_{FE}/P_{Pl} for groups G2 and G3 increased up to 0.28 and 0.40, respectively; while this increase in the P_{FE}/P_{Pl} ratio, for groups G4, G5 and G6 was up to 0.25, 0.31 and 0.43, respectively. As the results show, by increasing the effective length of

Table 4
Range of ratios α and λ for buckling modes in different groups.

Group	WD		LDB		LTB	
	α	λ	α	λ	α	λ
G1	0.051	101.2	0.051–0.162	101.2–126.8	0.195	132.9
G2	–	–	0.051–0.162	126.0–157.9	0.195	165.4
G3	–	–	0.051–0.162	150.8–189.0	0.162–0.195	189.0–198.1
G4	0.049–071	89.2–94.7	0.065–0.189	92.7–117.8	–	–
G5	0.048–0.057	111.2–114.1	0.048–0.185	111.2–147.4	–	–
G6	–	–	133.2–176.8	0.047–0.183	0.183	176.8

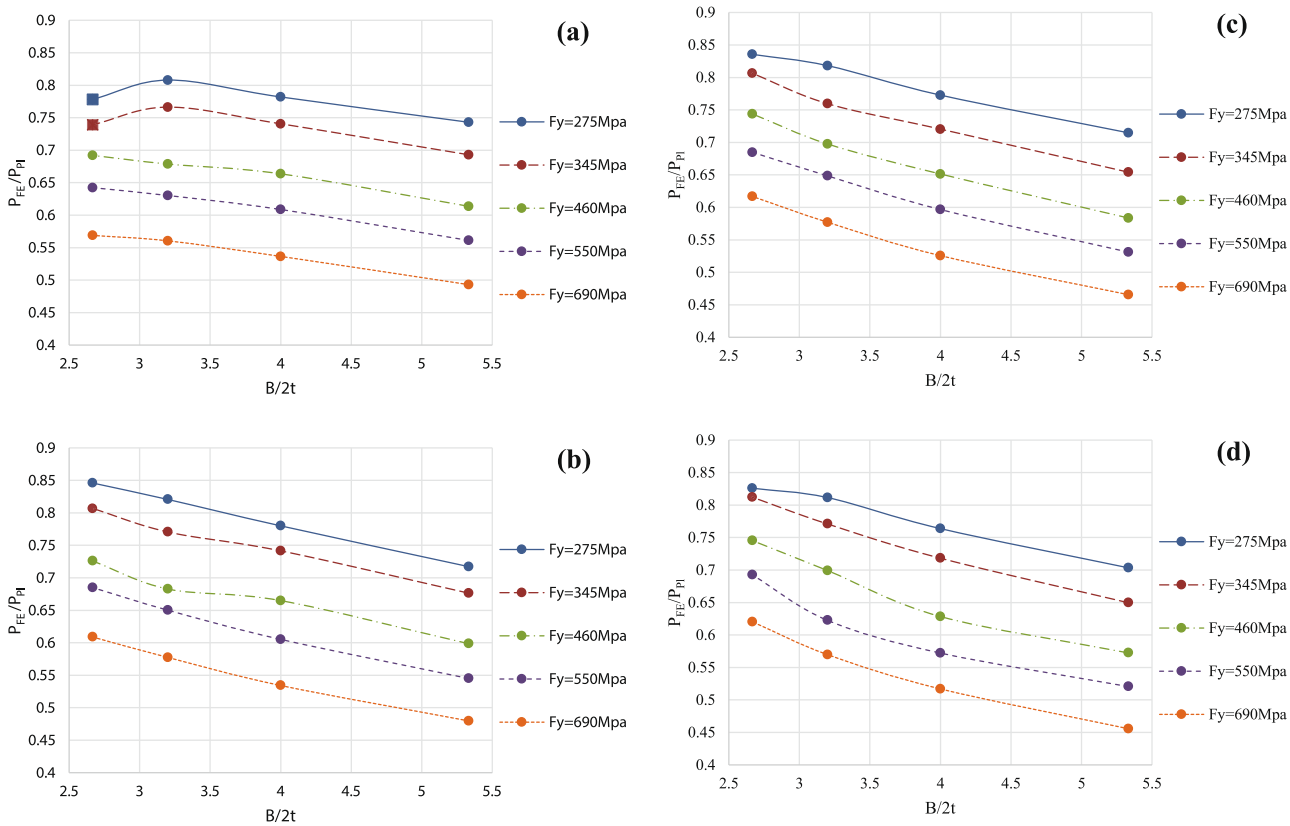

Fig. 8. Effects of flange slenderness and yield stress on the P_{FE}/P_{Pl} ratio for G1 specimens: (a) h/s = 56.7 (b) h/s = 42.5 (c) h/s = 34.0 (d) h/s = 28.3.

castellated beams, changing the grade of steel, has a greater impact on the consumed capacity of the beam cross section.

Another results which can be obtained by examining the failure loads of the modelled castellated steel beams is that, as expected, with the occurrence of local buckling in the beam, less of its capacity is used compared to the full plastic capacity. As can be seen from Fig. 8(a), the occurrence of WD mode in specimens with flange slenderness of 2.7 and yield stresses of 275 and 345 MPa (shown by the square symbol in the figure), caused a downward trend in P_{FE}/P_{Pl} ratios. Similar conclusions were observed for other specimens with WD mode in groups G4 and G5. Moreover, this should be noted that for specimens with similar characteristics in all groups G1-G6, changing the h/s ratio had little effect on P_{FE}/P_{Pl} values.

5. Comparison with design guides

In the following section, the performance of current design guides in estimating the ultimate failure load of castellated steel beams is examined. To the best of authors' knowledge, there are no design guides that consider LDB strength for beams, only design guides were found for calculating the LTB resistance of doubly symmetric I-sections. Therefore, three design codes comprising AS4100 [37], EC3 [26] and AISC [38] were considered and based on the LTB solutions provided in them, the ultimate buckling loads of all specimens were calculated. It should be mentioned that specimens with local buckling in the web (WD) are not considered. Hence, the ultimate loads estimated by the design Specifications were compared to the ultimate failure loads obtained from finite element analyzes. Fig. 9 plotted the P_{Code}/P_{FE} ratios for all 456 specimens that buckled in LTB or LDB mode. As it is clear from the figure, in estimating the ultimate buckling loads of castellated steel beams, the design codes make unsafe predictions for most specimens; however, it should be noted that web distortion was also included in the FE results, whereas this effect was not included in the codes' solutions. Moreover, it can be seen from Fig. 9, that the most unsafe predictions were related to AISC, followed by EC3 and AS4100, respectively.

A more detailed comparison between the performances of design codes in predicting the ultimate load of castellated steel beams, are illustrated in the bar chart of Fig. 10, the figure shows the frequency of the P_{Code}/P_{FE} ratios at different intervals. As it is clear from the figure, out of 456 specimens, Australian code provides conservative predictions for 167 specimens and unsafe predictions for 289 specimens. Moreover, it is concluded that AS4100 had very conservative predictions for 4

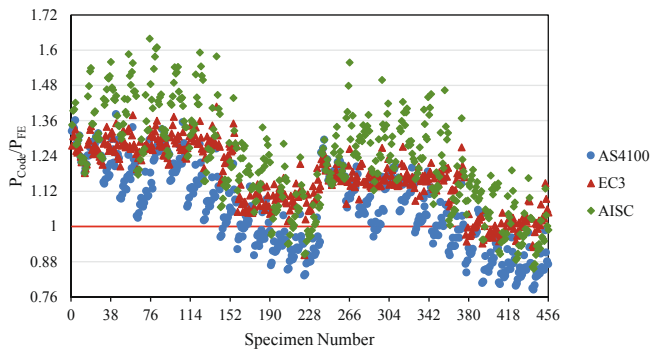

Fig. 9. Comparison between ultimate failure loads obtained from FEA and design codes.

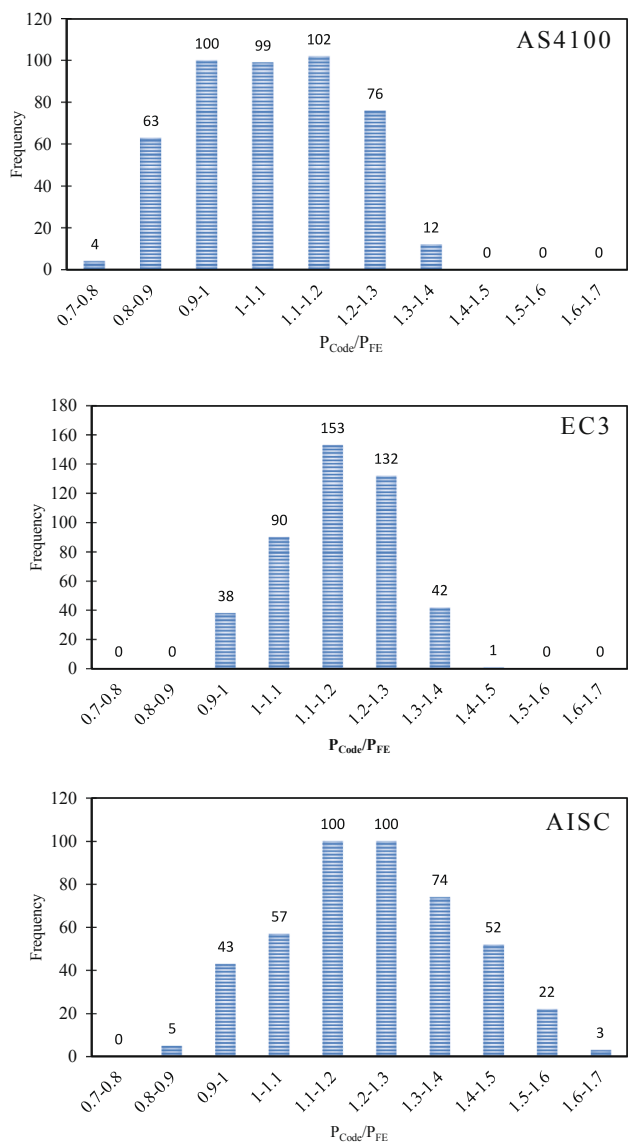

Fig. 10. Comparison between results of FEA and design codes.

specimens, with P_{Code}/P_{FE} ratios between 0.7 and 0.8; these specimens belonged to group G6, and had a flange thickness of 6 mm and yield stresses of 690 and 550 MPa.

On the other hand, AS4100 provided very unsafe predictions for 12 specimens, with P_{Code}/P_{FE} ratios greater than 1.3; most of these specimens had flange thicknesses of 10 and 12 mm and yield stresses of 275 and 345 MPa; therefore, it can be concluded that with increasing the flange slenderness and yield stress, Australian code offers more conservative results.

The European code EC3, provides more unsafe results than AS4100, such that only for 38 specimens (related to groups G3 and G6), the ratio of *PCode/PFE* was less than one. It can also be concluded that, EC3 provides the most unsafe predictions for specimens with slender flanges and mild steel (Fy = 275, 345 MPa), as well as for specimens with thick flanges and high-strength steel (Fy = 460, 550, 690 MPa). Besides, as shown in Fig. 10, EC3 predicts very unsafe results for 43 specimens with *PCode/PFE* ratios greater than 1.3.

The results of AISC code were more uncoservative than EC3 and AS4100 codes; in such a way that this code provided extremely unsafe predictions for 25 specimens, with *PCode/PFE* ratios greater than 1.5. On the other hand, AISC predicted conservative results for 48 specimens (related to groups G3 and G6), with *PCode/PFE* ratios of less than one. Most of these specimens had yield stresses of 690, 550 and 460 MPa and flange thicknesses of 6 and 8 mm. The results also showed that by increasing the yield stress and flange slenderness, AISC code provides more conservative predictions.

As mentioned before, most conservative predictions of all three codes were related to groups G3 and G6, on the other hand, according to Table 4, the highest λ ratios were observed in groups G3 and G6; therefore, it can be concluded that specimens with higher overall slenderness ratio provide more conservative results for all three codes, this conclusion is also confirmed by Fig. 11. The λ ratios against the P_{Code}/P_{FE} ratios were plotted in Fig. 11, as shown in the figure, by increasing λ ratio, for all three codes, a downward trend for P_{Code}/P_{FE} ratio is observed.

Moreover, the P_{Code}/P_{Pl} ratios of all specimens with LDB or LTB mode, were examined for all three mentioned codes. Based on the predictions of AISC code, this ratio was equal to one for 168 specimens, while according to the results of AS4100 and EC3 codes, this ratio was equal to one, for 43 and 11 specimens, respectively. Therefore, as mentioned before, AISC offers more unsafe predictions than AS4100 and EC3; which estimates the full plastic capacity for almost one-third of the specimens. All the results obtained in this study, including failure loads, failure modes, codes' predictions, as well as other parameters related to FE specimens in all groups, are presented in Appendix A.

6. Conclusions

In the current paper, an extensive numerical study was performed to investigate the buckling behavior of castellated steel beams, while the effects of web distortion on the ultimate loads were also considered. A nonlinear finite element model for analysis of simply supported castellated steel beams was developed, and then according to it, 480 specimens of castellated steel beams with different characteristics were modeled and analyzed. Three main variable parameters in this study included web slenderness, flange slenderness and steel yield stress. Moreover, the results obtained from finite element analysis were compared with the results of three design codes AS4100, EC3 and AISC, to examine the performance of current design guides in estimating the ultimate failure load of castellated steel beams. Consequently, the main conclusions of this study can be presented as follows:

- Since thick flanges and slender web were considered in this study, as expected, most modelled castellated beams buckled in LDB mode; out of 480 specimens, the buckling mode of 436 specimens was LDB mode.
- By decreasing the overall slenderness of beam, flange slenderness and steel grade, and also with increasing the web slenderness, the probability of occurrence of WD mode increases; the buckling mode of 24 specimens in this study was WD.

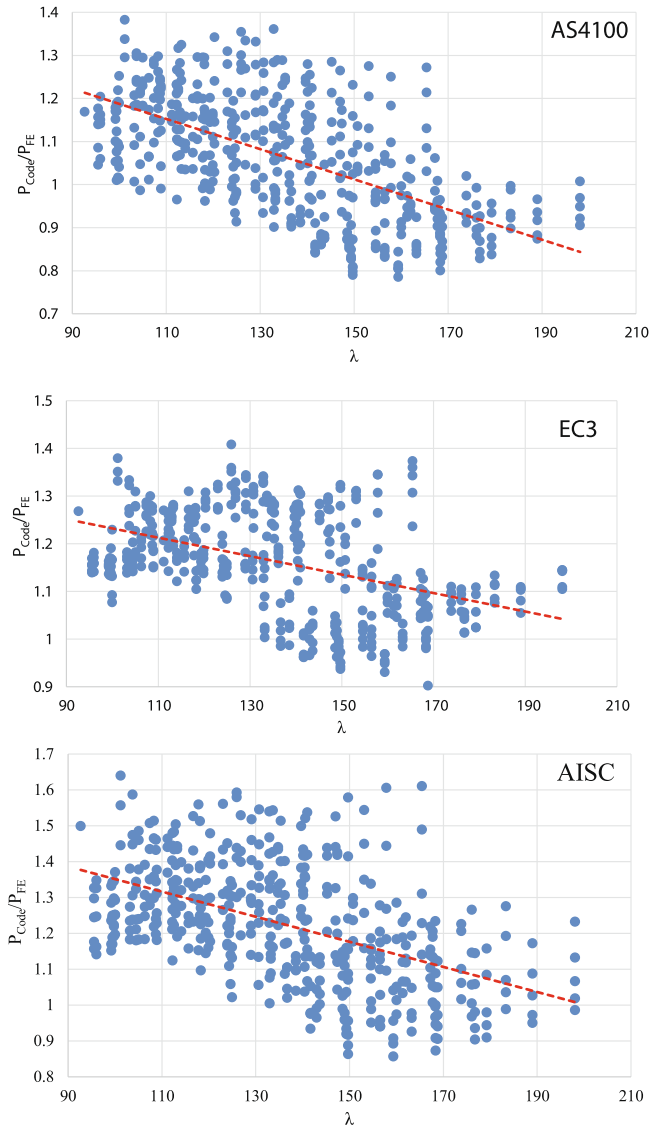

Fig. 11. Comparison between results of FEA and design codes with increasing overall slenderness ratio.

- In contrast to WD mode, LTB mode is more likely as the overall slenderness of beam, flange slenderness and steel grade increases, and web slenderness decreases; the buckling mode of 20 specimens in this study was LTB.
- By decreasing the flange slenderness and yield stress, more capacity of beam cross section is consumed compared to the full plastic capacity. Moreover, by increasing the effective length of beams, changing the steel grade, has a greater impact on the consumed capacity of beam cross section.
- Existing design solutions in AS4100, EC3 and AISC, provide unsafe predictions for the ultimate load of castellated steel beams; the most unsafe predictions were related to AISC, followed by EC3 and AS4100, respectively.
- As the flange slenderness and yield stress increase, AS4100 and AISC provide more conservative predictions.
- EC3 offers more unsafe predictions, for mild steel specimens with slender flanges, as well as for high-strength steel specimens with thick flanges.
- By increasing the overall slenderness of beams, all three codes examined in this study, provide more conservative results.

Declaration of Competing Interest

The authors declare that they have no known competing financial interests or personal relationships that could have appeared to influence the work reported in this paper.

Appendix A. The database of FE samples. Failure load and buckling mode of FE samples.

Sample	F_y	λ	B/2t	h/s	(h/s)/(B/t)	mode	P_{FE}	P_{FE}/P_{px}
S1	275	113.27332	5.3333333	56.666667	5.3125	LDB	19.4	0.7430009
S2	275	120.30383	5.3333333	42.5	3.984375	LDB	20.2	0.717205
S3	275	126.84184	5.3333333	34	3.1875	LDB	21.6	0.7147716
S4	275	132.91782	5.3333333	28.333333	2.65625	LTB	22.7	0.7033525
S5	275	107.40897	4	56.666667	7.0833333	LDB	25.5	0.7819734
S6	275	112.9433	4	42.5	5.3125	LDB	27	0.7800187
S7	275	118.14959	4	34	4.25	LDB	28.3	0.7728164
S8	275	123.04235	4	28.333333	3.5416667	LDB	29.5	0.7637727
S9	275	103.72917	3.2	56.666667	8.8541667	LDB	31.6	0.8079545
S10	275	108.28052	3.2	42.5	6.640625	LDB	33.7	0.8206169
S11	275	112.59739	3.2	34	5.3125	LDB	35.2	0.8181818
S12	275	116.68653	3.2	28.333333	4.4270833	LDB	36.5	0.8115119
S13	275	101.20073	2.6666667	56.666667	10.625	WD	35.5	0.7782656
S14	275	105.05427	2.6666667	42.5	7.96875	LDB	40.2	0.8459378
S15	275	108.73192	2.6666667	34	6.375	LDB	41.3	0.8355555

(*continued on next page*)

(*continued*)

Sample	F_y	λ	B/2t	h/s	(h/s)/(B/t)	mode	P_{FE}	P_{FE}/P_{px}
S16	275	112.23643	2.6666667	28.333333	5.3125	LDB	42.4	0.8259445
S17	345	113.27332	5.3333333	56.666667	5.3125	LDB	22.7	0.6929901
S18	345	120.30383	5.3333333	42.5	3.984375	LDB	23.9	0.6763998
S19	345	126.84184	5.3333333	34	3.1875	LDB	24.8	0.6541522
S20	345	132.91782	5.3333333	28.333333	2.65625	LTB	26.3	0.6495559
S21	345	107.40897	4	56.666667	7.0833333	LDB	30.3	0.7406415
S22	345	112.9433	4	42.5	5.3125	LDB	32.2	0.7414992
S23	345	118.14959	4	34	4.25	LDB	33.1	0.7204959
S24	345	123.04235	4	28.333333	3.5416667	LDB	34.8	0.7181827
S25	345	103.72917	3.2	56.666667	8.8541667	LDB	37.6	0.7663043
S26	345	108.28052	3.2	42.5	6.640625	LDB	39.7	0.7705745
S27	345	112.59739	3.2	34	5.3125	LDB	41	0.7596344
S28	345	116.68653	3.2	28.333333	4.4270833	LDB	43.5	0.7709121
S29	345	101.20073	2.6666667	56.666667	10.625	WD	42.3	0.7391855
S30	345	105.05427	2.6666667	42.5	7.96875	LDB	48.1	0.8068096
S31	345	108.73192	2.6666667	34	6.375	LDB	50	0.8063226
S32	345	112.23643	2.6666667	28.333333	5.3125	LDB	52.3	0.8120828
S33	460	113.27332	5.3333333	56.666667	5.3125	LDB	26.8	0.6136168
S34	460	120.30383	5.3333333	42.5	3.984375	LDB	28.2	0.5985714
S35	460	126.84184	5.3333333	34	3.1875	LDB	29.5	0.5835934
S36	460	132.91782	5.3333333	28.333333	2.65625	LTB	30.9	0.5723749
S37	460	107.40897	4	56.666667	7.0833333	LDB	36.2	0.6636441
S38	460	112.9433	4	42.5	5.3125	LDB	38.5	0.6649314
S39	460	118.14959	4	34	4.25	LDB	39.9	0.6513849
S40	460	123.04235	4	28.333333	3.5416667	LDB	40.6	0.6284099
S41	460	103.72917	3.2	56.666667	8.8541667	LDB	44.4	0.6786685
S42	460	108.28052	3.2	42.5	6.640625	LDB	46.9	0.6827446
S43	460	112.59739	3.2	34	5.3125	LDB	50.2	0.6975667
S44	460	116.68653	3.2	28.333333	4.4270833	LDB	52.6	0.6991375
S45	460	101.20073	2.6666667	56.666667	10.625	LDB	52.8	0.6920034
S46	460	105.05427	2.6666667	42.5	7.96875	LDB	57.7	0.7258771
S47	460	108.73192	2.6666667	34	6.375	LDB	61.5	0.7438326
S48	460	112.23643	2.6666667	28.333333	5.3125	LDB	64	0.745315
S49	550	113.27332	5.3333333	56.666667	5.3125	LDB	29.3	0.5610805
S50	550	120.30383	5.3333333	42.5	3.984375	LDB	30.7	0.5450048
S51	550	126.84184	5.3333333	34	3.1875	LDB	32.1	0.531115
S52	550	132.91782	5.3333333	28.333333	2.65625	LTB	33.6	0.5205429
S53	550	107.40897	4	56.666667	7.0833333	LDB	39.7	0.6087126
S54	550	112.9433	4	42.5	5.3125	LDB	41.9	0.6052367
S55	550	118.14959	4	34	4.25	LDB	43.7	0.5966798
S56	550	123.04235	4	28.333333	3.5416667	LDB	44.2	0.5721823
S57	550	103.72917	3.2	56.666667	8.8541667	LDB	49.3	0.6302557
S58	550	108.28052	3.2	42.5	6.640625	LDB	53.4	0.6501623
S59	550	112.59739	3.2	34	5.3125	LDB	55.8	0.6485021
S60	550	116.68653	3.2	28.333333	4.4270833	LDB	56	0.6225296
S61	550	101.20073	2.6666667	56.666667	10.625	LDB	58.6	0.6423431
S62	550	105.05427	2.6666667	42.5	7.96875	LDB	65.1	0.6849571
S63	550	108.73192	2.6666667	34	6.375	LDB	67.7	0.6848318
S64	550	112.23643	2.6666667	28.333333	5.3125	LDB	71.1	0.6925077
S65	690	113.27332	5.3333333	56.666667	5.3125	LDB	32.3	0.4930304
S66	690	120.30383	5.3333333	42.5	3.984375	LDB	33.9	0.4797061
S67	690	126.84184	5.3333333	34	3.1875	LDB	35.3	0.4655559
S68	690	132.91782	5.3333333	28.333333	2.65625	LTB	36.9	0.4556771
S69	690	107.40897	4	56.666667	7.0833333	LDB	43.9	0.5365373
S70	690	112.9433	4	42.5	5.3125	LDB	46.4	0.5342479
S71	690	118.14959	4	34	4.25	LDB	48.3	0.525679
S72	690	123.04235	4	28.333333	3.5416667	LDB	50.1	0.5169678
S73	690	103.72917	3.2	56.666667	8.8541667	LDB	55	0.560462
S74	690	108.28052	3.2	42.5	6.640625	LDB	59.5	0.5774457
S75	690	112.59739	3.2	34	5.3125	LDB	62.3	0.5771369
S76	690	116.68653	3.2	28.333333	4.4270833	LDB	64.3	0.5697661
S77	690	101.20073	2.6666667	56.666667	10.625	LDB	65.1	0.5688058
S78	690	105.05427	2.6666667	42.5	7.96875	LDB	72.6	0.6088813
S79	690	108.73192	2.6666667	34	6.375	LDB	76.5	0.6168368
S80	690	112.23643	2.6666667	28.333333	5.3125	LDB	79.9	0.6203195
S81	275	140.98544	5.3333333	56.666667	5.3125	LDB	13.9	0.6506577
S82	275	149.73596	5.3333333	42.5	3.984375	LDB	14.6	0.6335706
S83	275	157.87348	5.3333333	34	3.1875	LDB	15.4	0.6228514
S84	275	165.43595	5.3333333	28.333333	2.65625	LTB	16.4	0.621071
S85	275	133.6864	4	56.666667	7.0833333	LDB	18.7	0.7008798
S86	275	140.57468	4	42.5	5.3125	LDB	20	0.7061898
S87	275	147.05469	4	34	4.25	LDB	20.8	0.69423
S88	275	153.14445	4	28.333333	3.5416667	LDB	21.8	0.6898407
S89	275	129.10634	3.2	56.666667	8.8541667	LDB	24	0.75
S90	275	134.77117	3.2	42.5	6.640625	LDB	25.6	0.7619048
S91	275	140.14415	3.2	34	5.3125	LDB	26.7	0.7585227

(*continued on next page*)

(*continued*)

Sample	F_y	λ	B/2t	h/s	(h/s)/(B/t)	mode	P_{FE}	P_{FE}/P_{px}
S92	275	145.2337	3.2	28.333333	4.4270833	LDB	27.7	0.7527174
S93	275	125.95932	2.6666667	56.666667	10.625	LDB	28.7	0.7690092
S94	275	130.75562	2.6666667	42.5	7.96875	LDB	30.9	0.7947326
S95	275	135.333	2.6666667	34	6.375	LDB	32.6	0.8061076
S96	275	139.69489	2.6666667	28.333333	5.3125	LDB	33.7	0.8023523
S97	345	140.98544	5.3333333	56.666667	5.3125	LDB	15.7	0.5858022
S98	345	149.73596	5.3333333	42.5	3.984375	LDB	16.5	0.5707418
S99	345	157.87348	5.3333333	34	3.1875	LDB	17.3	0.5577292
S100	345	165.43595	5.3333333	28.333333	2.65625	LTB	18.3	0.5524107
S101	345	133.6864	4	56.666667	7.0833333	LDB	21.7	0.6482989
S102	345	140.57468	4	42.5	5.3125	LDB	22.9	0.6445261
S103	345	147.05469	4	34	4.25	LDB	23.8	0.633185
S104	345	153.14445	4	28.333333	3.5416667	LDB	24.9	0.6280659
S105	345	129.10634	3.2	56.666667	8.8541667	LDB	27.5	0.6850091
S106	345	134.77117	3.2	42.5	6.640625	LDB	29.4	0.6974638
S107	345	140.14415	3.2	34	5.3125	LDB	30.8	0.6974638
S108	345	145.2337	3.2	28.333333	4.4270833	LDB	32.1	0.6952977
S109	345	125.95932	2.6666667	56.666667	10.625	LDB	33.2	0.7090899
S110	345	130.75562	2.6666667	42.5	7.96875	LDB	35.9	0.7359878
S111	345	135.333	2.6666667	34	6.375	LDB	37.9	0.7470131
S112	345	139.69489	2.6666667	28.333333	5.3125	LDB	39.4	0.7477304
S113	460	140.98544	5.3333333	56.666667	5.3125	LDB	18	0.5037153
S114	460	149.73596	5.3333333	42.5	3.984375	LDB	18.8	0.4877248
S115	460	157.87348	5.3333333	34	3.1875	LDB	19.7	0.4763265
S116	460	165.43595	5.3333333	28.333333	2.65625	LTB	20.8	0.4709075
S117	460	133.6864	4	56.666667	7.0833333	LDB	24.9	0.5579255
S118	460	140.57468	4	42.5	5.3125	LDB	25.7	0.5424996
S119	460	147.05469	4	34	4.25	LDB	27.4	0.5467207
S120	460	153.14445	4	28.333333	3.5416667	LDB	28.5	0.539153
S121	460	129.10634	3.2	56.666667	8.8541667	LDB	31.9	0.5959579
S122	460	134.77117	3.2	42.5	6.640625	LDB	34.2	0.6085016
S123	460	140.14415	3.2	34	5.3125	LDB	35.7	0.6063179
S124	460	145.2337	3.2	28.333333	4.4270833	LDB	37.1	0.6026997
S125	460	125.95932	2.6666667	56.666667	10.625	LDB	39.2	0.627929
S126	460	130.75562	2.6666667	42.5	7.96875	LDB	42.1	0.6473208
S127	460	135.333	2.6666667	34	6.375	LDB	44.7	0.6607814
S128	460	139.69489	2.6666667	28.333333	5.3125	LDB	46.5	0.6618552
S129	550	140.98544	5.3333333	56.666667	5.3125	LDB	19.3	0.4517156
S130	550	149.73596	5.3333333	42.5	3.984375	LDB	20.2	0.438292
S131	550	157.87348	5.3333333	34	3.1875	LDB	21.1	0.4266936
S132	550	165.43595	5.3333333	28.333333	2.65625	LTB	22.2	0.420359
S133	550	133.6864	4	56.666667	7.0833333	LDB	26.8	0.5022348
S134	550	140.57468	4	42.5	5.3125	LDB	28.2	0.4978638
S135	550	147.05469	4	34	4.25	LDB	29.4	0.4906337
S136	550	153.14445	4	28.333333	3.5416667	LDB	30.6	0.4841542
S137	550	129.10634	3.2	56.666667	8.8541667	LDB	34.5	0.5390625
S138	550	134.77117	3.2	42.5	6.640625	LDB	37	0.5505952
S139	550	140.14415	3.2	34	5.3125	LDB	38.7	0.5497159
S140	550	145.2337	3.2	28.333333	4.4270833	LDB	40.1	0.544837
S141	550	125.95932	2.6666667	56.666667	10.625	LDB	41.8	0.5600102
S142	550	130.75562	2.6666667	42.5	7.96875	LDB	46.1	0.5928345
S143	550	135.333	2.6666667	34	6.375	LDB	48.5	0.5996353
S144	550	139.69489	2.6666667	28.333333	5.3125	LDB	50.4	0.5999786
S145	690	140.98544	5.3333333	56.666667	5.3125	LDB	20.9	0.3899129
S146	690	149.73596	5.3333333	42.5	3.984375	LDB	21.8	0.3770355
S147	690	157.87348	5.3333333	34	3.1875	LDB	22.8	0.367521
S148	690	165.43595	5.3333333	28.333333	2.65625	LTB	23.9	0.3607272
S149	690	133.6864	4	56.666667	7.0833333	LDB	29.2	0.4361827
S150	690	140.57468	4	42.5	5.3125	LDB	30.7	0.4320295
S151	690	147.05469	4	34	4.25	LDB	31.9	0.4243404
S152	690	153.14445	4	28.333333	3.5416667	LDB	33.2	0.4187106
S153	690	129.10634	3.2	56.666667	8.8541667	LDB	37.7	0.4695426
S154	690	134.77117	3.2	42.5	6.640625	LDB	40.3	0.4780236
S155	690	140.14415	3.2	34	5.3125	LDB	42.1	0.4766757
S156	690	145.2337	3.2	28.333333	4.4270833	LDB	43.6	0.472196
S157	690	125.95932	2.6666667	56.666667	10.625	LDB	45.9	0.4901691
S158	690	130.75562	2.6666667	42.5	7.96875	LDB	50.3	0.5156015
S159	690	135.333	2.6666667	34	6.375	LDB	53	0.5223179
S160	690	139.69489	2.6666667	28.333333	5.3125	LDB	55	0.521893
S161	275	168.7776	5.3333333	56.8	5.325	LDB	12.9	0.7115389
S162	275	179.268	5.3333333	42.6	3.99375	LDB	13.2	0.6748794
S163	275	189.02255	5.3333333	34.08	3.195	LDB	14.1	0.6718003
S164	275	198.08692	5.3333333	28.4	2.6625	LTB	14.8	0.6601923
S165	275	160.02717	4	56.8	7.1	LDB	17.5	0.7729706
S166	275	168.28602	4	42.6	5.325	LDB	18.8	0.7822025
S167	275	176.05467	4	34.08	4.26	LDB	19.2	0.7550298

(*continued on next page*)

(*continued*)

Sample	F_y	λ	B/2t	h/s	(h/s)/(B/t)	mode	P_{FE}	P_{FE}/P_{px}
S168	275	183.35482	4	28.4	3.55	LDB	20.3	0.7567785
S169	275	154.536	3.2	56.8	8.875	LDB	22.9	0.8434184
S170	275	161.3286	3.2	42.6	6.65625	LDB	24	0.8417498
S171	275	167.77071	3.2	34.08	5.325	LDB	25.1	0.8402332
S172	275	173.87251	3.2	28.4	4.4375	LDB	25.9	0.8292436
S173	275	150.76276	2.6666667	56.8	10.65	LDB	26.9	0.8495409
S174	275	156.51437	2.6666667	42.6	7.9875	LDB	29.3	0.8881193
S175	275	162.00305	2.6666667	34.08	6.39	LDB	30.4	0.8858333
S176	275	167.23293	2.6666667	28.4	5.325	LDB	31.3	0.8781066
S177	345	168.7776	5.3333333	56.8	5.325	LDB	13.8	0.6067386
S178	345	179.268	5.3333333	42.6	3.99375	LDB	14.1	0.5746256
S179	345	189.02255	5.3333333	34.08	3.195	LDB	15.2	0.577269
S180	345	198.08692	5.3333333	28.4	2.6625	LTB	16.1	0.572464
S181	345	160.02717	4	56.8	7.1	LDB	19	0.6689477
S182	345	168.28602	4	42.6	5.325	LDB	20.6	0.6831911
S183	345	176.05467	4	34.08	4.26	LDB	21.2	0.6645265
S184	345	183.35482	4	28.4	3.55	LDB	21.7	0.6448313
S185	345	154.536	3.2	56.8	8.875	LDB	24.4	0.7163265
S186	345	161.3286	3.2	42.6	6.65625	LDB	27	0.75483
S187	345	167.77071	3.2	34.08	5.325	LDB	28.4	0.7578061
S188	345	173.87251	3.2	28.4	4.4375	LDB	29.1	0.7426582
S189	345	150.76276	2.6666667	56.8	10.65	LDB	30.6	0.7703127
S190	345	156.51437	2.6666667	42.6	7.9875	LDB	32.4	0.7828207
S191	345	162.00305	2.6666667	34.08	6.39	LDB	34.6	0.8036522
S192	345	167.23293	2.6666667	28.4	5.325	LDB	36.7	0.8206965
S193	460	168.7776	5.3333333	56.8	5.325	LDB	14.9	0.4913264
S194	460	179.268	5.3333333	42.6	3.99375	LDB	15.6	0.476817
S195	460	189.02255	5.3333333	34.08	3.195	LDB	16.1	0.4585871
S196	460	198.08692	5.3333333	28.4	2.6625	LTB	17.1	0.4560156
S197	460	160.02717	4	56.8	7.1	LDB	21.4	0.5650847
S198	460	168.28602	4	42.6	5.325	LDB	22.1	0.5497035
S199	460	176.05467	4	34.08	4.26	LDB	23	0.5407114
S200	460	183.35482	4	28.4	3.55	LDB	24.2	0.5393405
S201	460	154.536	3.2	56.8	8.875	LDB	28.2	0.6209142
S202	460	161.3286	3.2	42.6	6.65625	LDB	29.7	0.6227348
S203	460	167.77071	3.2	34.08	5.325	LDB	30.2	0.604377
S204	460	173.87251	3.2	28.4	4.4375	LDB	32.4	0.6201579
S205	460	150.76276	2.6666667	56.8	10.65	LDB	35.1	0.6626955
S206	460	156.51437	2.6666667	42.6	7.9875	LDB	37.8	0.6849681
S207	460	162.00305	2.6666667	34.08	6.39	LDB	39.8	0.6933242
S208	460	167.23293	2.6666667	28.4	5.325	LDB	41.3	0.6926723
S209	550	168.7776	5.3333333	56.8	5.325	LDB	15.4	0.424717
S210	550	179.268	5.3333333	42.6	3.99375	LDB	16.2	0.4141306
S211	550	189.02255	5.3333333	34.08	3.195	LDB	17	0.404986
S212	550	198.08692	5.3333333	28.4	2.6625	LTB	17.9	0.3992379
S213	550	160.02717	4	56.8	7.1	LDB	22.2	0.4902842
S214	550	168.28602	4	42.6	5.325	LDB	23.3	0.4847159
S215	550	176.05467	4	34.08	4.26	LDB	24.2	0.475826
S216	550	183.35482	4	28.4	3.55	LDB	25	0.4659966
S217	550	154.536	3.2	56.8	8.875	LDB	29.4	0.5414083
S218	550	161.3286	3.2	42.6	6.65625	LDB	31.2	0.5471374
S219	550	167.77071	3.2	34.08	5.325	LDB	32.5	0.5439757
S220	550	173.87251	3.2	28.4	4.4375	LDB	33.6	0.5378878
S221	550	150.76276	2.6666667	56.8	10.65	LDB	36.4	0.5747823
S222	550	156.51437	2.6666667	42.6	7.9875	LDB	39.9	0.6047092
S223	550	162.00305	2.6666667	34.08	6.39	LDB	41.5	0.6046395
S224	550	167.23293	2.6666667	28.4	5.325	LDB	43.2	0.6059777
S225	690	168.7776	5.3333333	56.8	5.325	LDB	16	0.3517325
S226	690	179.268	5.3333333	42.6	3.99375	LDB	16.8	0.3423301
S227	690	189.02255	5.3333333	34.08	3.195	LTB	17.4	0.3304106
S228	690	198.08692	5.3333333	28.4	2.6625	LTB	18.5	0.3289001
S229	690	160.02717	4	56.8	7.1	LDB	23.1	0.4066498
S230	690	168.28602	4	42.6	5.325	LDB	24	0.3979754
S231	690	176.05467	4	34.08	4.26	LDB	25.1	0.3933871
S232	690	183.35482	4	28.4	3.55	LDB	26.2	0.389276
S233	690	154.536	3.2	56.8	8.875	LDB	30.4	0.4462362
S234	690	161.3286	3.2	42.6	6.65625	LDB	32.2	0.4501023
S235	690	167.77071	3.2	34.08	5.325	LDB	34	0.4536163
S236	690	173.87251	3.2	28.4	4.4375	LDB	35.1	0.4478918
S237	690	150.76276	2.6666667	56.8	10.65	LDB	38.2	0.4808161
S238	690	156.51437	2.6666667	42.6	7.9875	LDB	41.4	0.5001354
S239	690	162.00305	2.6666667	34.08	6.39	LDB	43.6	0.5063473
S240	690	167.23293	2.6666667	28.4	5.325	LDB	44.4	0.4964431
S241	275	99.997794	6.0833333	66.533333	5.4684932	LDB	28.2	0.7988098
S242	275	106.35367	6.0833333	49.9	4.1013699	LDB	30.6	0.8017681
S243	275	112.27709	6.0833333	39.92	3.2810959	LDB	32.4	0.7896896

(*continued on next page*)

(*continued*)

Sample	F_y	λ	B/2t	h/s	(h/s)/(B/t)	mode	P_{FE}	P_{FE}/P_{px}
S244	275	117.80301	6.0833333	33.266667	2.7342466	LDB	33.9	0.772352
S245	275	94.734348	4.5625	66.533333	7.2913242	WD	35.4	0.8039909
S246	275	99.749301	4.5625	49.9	5.4684932	LDB	39.3	0.8391227
S247	275	104.47486	4.5625	39.92	4.3747945	LDB	41	0.825965
S248	275	108.92919	4.5625	33.266667	3.6456621	LDB	42.7	0.8142145
S249	275	91.429402	3.65	66.533333	9.1141553	WD	40.2	0.7619407
S250	275	95.563185	3.65	49.9	6.8356164	LDB	48	0.8647706
S251	275	99.489415	3.65	39.92	5.4684932	LDB	49.8	0.854905
S252	275	103.21795	3.65	33.266667	4.5570776	LDB	51.6	0.8459276
S253	275	89.157407	3.0416667	66.533333	10.936986	WD	43.2	0.7025361
S254	275	92.665435	3.0416667	49.9	8.2027397	WD	55.7	0.8678728
S255	275	96.017389	3.0416667	39.92	6.5621918	LDB	58.6	0.8763491
S256	275	99.218639	3.0416667	33.266667	5.4684932	LDB	60.4	0.8683558
S257	345	99.997794	6.0833333	66.533333	5.4684932	LDB	35.4	0.7993025
S258	345	106.35367	6.0833333	49.9	4.1013699	LDB	37.6	0.7852877
S259	345	112.27709	6.0833333	39.92	3.2810959	LDB	39.3	0.763515
S260	345	117.80301	6.0833333	33.266667	2.7342466	LDB	41.1	0.7463989
S261	345	94.734348	4.5625	66.533333	7.2913242	WD	42.5	0.7693969
S262	345	99.749301	4.5625	49.9	5.4684932	LDB	48.2	0.8203394
S263	345	104.47486	4.5625	39.92	4.3747945	LDB	50.3	0.8077173
S264	345	108.92919	4.5625	33.266667	3.6456621	LDB	52.4	0.7964451
S265	345	91.429402	3.65	66.533333	9.1141553	WD	47.7	0.7206545
S266	345	95.563185	3.65	49.9	6.8356164	LDB	59.2	0.8501489
S267	345	99.489415	3.65	39.92	5.4684932	LDB	61.5	0.8415447
S268	345	103.21795	3.65	33.266667	4.5570776	LDB	63.4	0.8284882
S269	345	89.157407	3.0416667	66.533333	10.936986	WD	51.3	0.6649911
S270	345	92.665435	3.0416667	49.9	8.2027397	WD	66.6	0.8271584
S271	345	96.017389	3.0416667	39.92	6.5621918	LDB	72.2	0.8606575
S272	345	99.218639	3.0416667	33.266667	5.4684932	LDB	74.6	0.8548958
S273	460	99.997794	6.0833333	66.533333	5.4684932	LDB	43.1	0.7298715
S274	460	106.35367	6.0833333	49.9	4.1013699	LDB	45.9	0.7189768
S275	460	112.27709	6.0833333	39.92	3.2810959	LDB	46.4	0.6760896
S276	460	117.80301	6.0833333	33.266667	2.7342466	LDB	47.1	0.6415217
S277	460	94.734348	4.5625	66.533333	7.2913242	WD	53	0.7196124
S278	460	99.749301	4.5625	49.9	5.4684932	LDB	60.4	0.7709829
S279	460	104.47486	4.5625	39.92	4.3747945	LDB	61.8	0.7442882
S280	460	108.92919	4.5625	33.266667	3.6456621	LDB	63.7	0.7261482
S281	460	91.429402	3.65	66.533333	9.1141553	WD	58.4	0.6617331
S282	460	95.563185	3.65	49.9	6.8356164	LDB	74.6	0.8034769
S283	460	99.489415	3.65	39.92	5.4684932	LDB	78	0.8004938
S284	460	103.21795	3.65	33.266667	4.5570776	LDB	80.1	0.7850383
S285	460	89.157407	3.0416667	66.533333	10.936986	WD	59.9	0.5823533
S286	460	92.665435	3.0416667	49.9	8.2027397	WD	85.4	0.7954879
S287	460	96.017389	3.0416667	39.92	6.5621918	LDB	89.7	0.8019492
S288	460	99.218639	3.0416667	33.266667	5.4684932	LDB	94.2	0.8096299
S289	550	99.997794	6.0833333	66.533333	5.4684932	LDB	47.4	0.6713402
S290	550	106.35367	6.0833333	49.9	4.1013699	LDB	48.1	0.6301478
S291	550	112.27709	6.0833333	39.92	3.2810959	LDB	50.4	0.614203
S292	550	117.80301	6.0833333	33.266667	2.7342466	LDB	53.5	0.6094518
S293	550	94.734348	4.5625	66.533333	7.2913242	WD	60.1	0.6824838
S294	550	99.749301	4.5625	49.9	5.4684932	LDB	66.4	0.7088772
S295	550	104.47486	4.5625	39.92	4.3747945	LDB	69.3	0.6980412
S296	550	108.92919	4.5625	33.266667	3.6456621	LDB	72.6	0.6921776
S297	550	91.429402	3.65	66.533333	9.1141553	WD	65.9	0.6245261
S298	550	95.563185	3.65	49.9	6.8356164	LDB	83.7	0.7539719
S299	550	99.489415	3.65	39.92	5.4684932	LDB	86.8	0.7450377
S300	550	103.21795	3.65	33.266667	4.5570776	LDB	88.4	0.7246124
S301	550	89.157407	3.0416667	66.533333	10.936986	WD	70.8	0.5756893
S302	550	92.665435	3.0416667	49.9	8.2027397	WD	97.7	0.7611415
S303	550	96.017389	3.0416667	39.92	6.5621918	LDB	100.9	0.7544678
S304	550	99.218639	3.0416667	33.266667	5.4684932	LDB	108.3	0.7785011
S305	690	99.997794	6.0833333	66.533333	5.4684932	LDB	51.2	0.5780266
S306	690	106.35367	6.0833333	49.9	4.1013699	LDB	53.1	0.554505
S307	690	112.27709	6.0833333	39.92	3.2810959	LDB	58.2	0.5653508
S308	690	117.80301	6.0833333	33.266667	2.7342466	LDB	59.9	0.5439087
S309	690	94.734348	4.5625	66.533333	7.2913242	WD	69.1	0.6254744
S310	690	99.749301	4.5625	49.9	5.4684932	LDB	73	0.6212114
S311	690	104.47486	4.5625	39.92	4.3747945	LDB	77.7	0.6238532
S312	690	108.92919	4.5625	33.266667	3.6456621	LDB	80.6	0.6125331
S313	690	91.429402	3.65	66.533333	9.1141553	WD	74.9	0.5657969
S314	690	95.563185	3.65	49.9	6.8356164	LDB	92.9	0.6670509
S315	690	99.489415	3.65	39.92	5.4684932	LDB	98.7	0.6752883
S316	690	103.21795	3.65	33.266667	4.5570776	LDB	102.1	0.6671029
S317	690	89.157407	3.0416667	66.533333	10.936986	WD	80.3	0.520456
S318	690	92.665435	3.0416667	49.9	8.2027397	LDB	104.8	0.6507973
S319	690	96.017389	3.0416667	39.92	6.5621918	LDB	118.1	0.7039034

(*continued on next page*)

(*continued*)

Sample	F_y	λ	B/2t	h/s	(h/s)/(B/t)	mode	P_{FE}	P_{FE}/P_{px}
S320	690	99.218639	3.0416667	33.266667	5.4684932	LDB	121.8	0.6978975
S321	275	124.94675	6.0833333	67.8	5.5726027	LDB	22.7	0.7674476
S322	275	132.97764	6.0833333	50.85	4.1794521	LDB	23.8	0.743425
S323	275	140.45648	6.0833333	40.68	3.3435616	LDB	24.9	0.722799
S324	275	147.42852	6.0833333	33.9	2.7863014	LDB	26	0.7048967
S325	275	118.29498	4.5625	67.8	7.430137	LDB	30.1	0.816706
S326	275	124.63719	4.5625	50.85	5.5726027	LDB	31.6	0.805266
S327	275	130.60925	4.5625	40.68	4.4580822	LDB	32.5	0.7807243
S328	275	136.23488	4.5625	33.9	3.7150685	LDB	33.7	0.7656596
S329	275	114.11597	3.65	67.8	9.2876712	WD	36	0.8157038
S330	275	119.34748	3.65	50.85	6.9657534	LDB	38.7	0.8327704
S331	275	124.31312	3.65	40.68	5.5726027	LDB	40.7	0.8338607
S332	275	129.02586	3.65	33.9	4.6438356	LDB	41.9	0.81921
S333	275	111.24192	3.0416667	67.8	11.145205	WD	40.3	0.7838413
S334	275	115.68413	3.0416667	50.85	8.3589041	LDB	46.4	0.8640099
S335	275	119.92615	3.0416667	40.68	6.6871233	LDB	48.3	0.8626123
S336	275	123.97515	3.0416667	33.9	5.5726027	LDB	50	0.8578929
S337	345	124.94675	6.0833333	67.8	5.5726027	LDB	26.2	0.7060537
S338	345	132.97764	6.0833333	50.85	4.1794521	LDB	27.3	0.67973
S339	345	140.45648	6.0833333	40.68	3.3435616	LDB	28	0.6478729
S340	345	147.42852	6.0833333	33.9	2.7863014	LDB	28.6	0.6180616
S341	345	118.29498	4.5625	67.8	7.430137	LDB	33.3	0.7202066
S342	345	124.63719	4.5625	50.85	5.5726027	LDB	36.6	0.7434418
S343	345	130.60925	4.5625	40.68	4.4580822	LDB	37.6	0.7199723
S344	345	136.23488	4.5625	33.9	3.7150685	LDB	39.4	0.7135356
S345	345	114.11597	3.65	67.8	9.2876712	LDB	43.4	0.7838506
S346	345	119.34748	3.65	50.85	6.9657534	LDB	45.2	0.7752939
S347	345	124.31312	3.65	40.68	5.5726027	LDB	47.9	0.7822547
S348	345	129.02586	3.65	33.9	4.6438356	LDB	49.7	0.7745531
S349	345	111.24192	3.0416667	67.8	11.145205	WD	48.4	0.7503814
S350	345	115.68413	3.0416667	50.85	8.3589041	LDB	54	0.8015084
S351	345	119.92615	3.0416667	40.68	6.6871233	LDB	57.1	0.8128646
S352	345	123.97515	3.0416667	33.9	5.5726027	LDB	59.9	0.8192255
S353	460	124.94675	6.0833333	67.8	5.5726027	LDB	30.1	0.608365
S354	460	132.97764	6.0833333	50.85	4.1794521	LDB	31	0.5788909
S355	460	140.45648	6.0833333	40.68	3.3435616	LDB	32.2	0.5587904
S356	460	147.42852	6.0833333	33.9	2.7863014	LDB	34	0.5510689
S357	460	118.29498	4.5625	67.8	7.430137	LDB	40.3	0.653701
S358	460	124.63719	4.5625	50.85	5.5726027	LDB	42.4	0.6459412
S359	460	130.60925	4.5625	40.68	4.4580822	LDB	44	0.6318906
S360	460	136.23488	4.5625	33.9	3.7150685	LDB	45.9	0.6234382
S361	460	114.11597	3.65	67.8	9.2876712	LDB	50.7	0.6867724
S362	460	119.34748	3.65	50.85	6.9657534	LDB	53.3	0.685672
S363	460	124.31312	3.65	40.68	5.5726027	LDB	56.3	0.6895763
S364	460	129.02586	3.65	33.9	4.6438356	LDB	58.5	0.683773
S365	460	111.24192	3.0416667	67.8	11.145205	LDB	59.7	0.6941803
S366	460	115.68413	3.0416667	50.85	8.3589041	LDB	65.1	0.7246972
S367	460	119.92615	3.0416667	40.68	6.6871233	LDB	66.7	0.7121462
S368	460	123.97515	3.0416667	33.9	5.5726027	LDB	67.2	0.6892983
S369	550	124.94675	6.0833333	67.8	5.5726027	LDB	30.9	0.5223377
S370	550	132.97764	6.0833333	50.85	4.1794521	LDB	33.6	0.5247706
S371	550	140.45648	6.0833333	40.68	3.3435616	LDB	34.4	0.4992828
S372	550	147.42852	6.0833333	33.9	2.7863014	LDB	36.4	0.4934277
S373	550	118.29498	4.5625	67.8	7.430137	LDB	43.2	0.5860747
S374	550	124.63719	4.5625	50.85	5.5726027	LDB	45.9	0.5848372
S375	550	130.60925	4.5625	40.68	4.4580822	LDB	47.7	0.5729315
S376	550	136.23488	4.5625	33.9	3.7150685	LDB	48.4	0.5498209
S377	550	114.11597	3.65	67.8	9.2876712	LDB	53.7	0.6083791
S378	550	119.34748	3.65	50.85	6.9657534	LDB	57.8	0.621888
S379	550	124.31312	3.65	40.68	5.5726027	LDB	60.5	0.6197613
S380	550	129.02586	3.65	33.9	4.6438356	LDB	63.3	0.6188066
S381	550	111.24192	3.0416667	67.8	11.145205	LDB	64.4	0.626295
S382	550	115.68413	3.0416667	50.85	8.3589041	LDB	71	0.661042
S383	550	119.92615	3.0416667	40.68	6.6871233	LDB	74.6	0.6661581
S384	550	123.97515	3.0416667	33.9	5.5726027	LDB	75	0.6434197
S385	690	124.94675	6.0833333	67.8	5.5726027	LDB	34.2	0.4608213
S386	690	132.97764	6.0833333	50.85	4.1794521	LDB	36	0.4481736
S387	690	140.45648	6.0833333	40.68	3.3435616	LDB	36.7	0.4245881
S388	690	147.42852	6.0833333	33.9	2.7863014	LDB	39.1	0.4224862
S389	690	118.29498	4.5625	67.8	7.430137	LDB	46.7	0.5050097
S390	690	124.63719	4.5625	50.85	5.5726027	LDB	49.4	0.5017217
S391	690	130.60925	4.5625	40.68	4.4580822	LDB	51.2	0.4901939
S392	690	136.23488	4.5625	33.9	3.7150685	LDB	52.1	0.4717666
S393	690	114.11597	3.65	67.8	9.2876712	LDB	58.8	0.5309956
S394	690	119.34748	3.65	50.85	6.9657534	LDB	62.8	0.5385891
S395	690	124.31312	3.65	40.68	5.5726027	LDB	66.3	0.5413725

(*continued on next page*)

(*continued*)

Sample	F_y	λ	B/2t	h/s	(h/s)/(B/t)	mode	P_{FE}	P_{FE}/P_{px}
S396	690	129.02586	3.65	33.9	4.6438356	LDB	66.6	0.5189662
S397	690	111.24192	3.0416667	67.8	11.145205	LDB	68.9	0.5341041
S398	690	115.68413	3.0416667	50.85	8.3589041	LDB	77.5	0.5751565
S399	690	119.92615	3.0416667	40.68	6.6871233	LDB	81.4	0.5793973
S400	690	123.97515	3.0416667	33.9	5.5726027	LDB	84.5	0.5778344
S401	275	149.71939	6.0833333	68.266667	5.6109589	LDB	20.4	0.8080572
S402	275	159.38148	6.0833333	51.2	4.2082192	LDB	22.2	0.8121215
S403	275	168.37694	6.0833333	40.96	3.3665753	LDB	22.6	0.7680312
S404	275	176.76066	6.0833333	34.133333	2.8054795	LDB	23.3	0.7393078
S405	275	141.71599	4.5625	68.266667	7.4812785	LDB	27.7	0.8808926
S406	275	149.34887	4.5625	51.2	5.6109589	LDB	28.9	0.8628511
S407	275	156.53444	4.5625	40.96	4.4887671	LDB	30.1	0.846889
S408	275	163.30157	4.5625	34.133333	3.7406393	LDB	31.3	0.8326665
S409	275	136.68677	3.65	68.266667	9.3515982	LDB	34.1	0.9057997
S410	275	142.98453	3.65	51.2	7.0136986	LDB	35.4	0.8927422
S411	275	148.96082	3.65	40.96	5.6109589	LDB	36.7	0.8809427
S412	275	154.63147	3.65	34.133333	4.6757991	LDB	37.9	0.8679376
S413	275	133.2275	3.0416667	68.266667	11.221918	LDB	40.3	0.9190742
S414	275	138.57622	3.0416667	51.2	8.4164384	LDB	41.8	0.9123791
S415	275	143.68279	3.0416667	40.96	6.7331507	LDB	42.9	0.8978632
S416	275	148.556	3.0416667	34.133333	5.6109589	LDB	44.4	0.8925354
S417	345	149.71939	6.0833333	68.266667	5.6109589	LDB	23.2	0.73251
S418	345	159.38148	6.0833333	51.2	4.2082192	LDB	24.2	0.7056624
S419	345	168.37694	6.0833333	40.96	3.3665753	LDB	24.6	0.6663757
S420	345	176.76066	6.0833333	34.133333	2.8054795	LTB	25.2	0.6373581
S421	345	141.71599	4.5625	68.266667	7.4812785	LDB	31.5	0.798486
S422	345	149.34887	4.5625	51.2	5.6109589	LDB	32.8	0.7805944
S423	345	156.53444	4.5625	40.96	4.4887671	LDB	34.4	0.7714931
S424	345	163.30157	4.5625	34.133333	3.7406393	LDB	35.6	0.7549016
S425	345	136.68677	3.65	68.266667	9.3515982	LDB	39.8	0.8427029
S426	345	142.98453	3.65	51.2	7.0136986	LDB	42.1	0.8462886
S427	345	148.96082	3.65	40.96	5.6109589	LDB	43.9	0.8399621
S428	345	154.63147	3.65	34.133333	4.6757991	LDB	44.8	0.8177883
S429	345	133.2275	3.0416667	68.266667	11.221918	LDB	48.2	0.8762059
S430	345	138.57622	3.0416667	51.2	8.4164384	LDB	50.6	0.8803658
S431	345	143.68279	3.0416667	40.96	6.7331507	LDB	52.9	0.8825151
S432	345	148.556	3.0416667	34.133333	5.6109589	LDB	54.4	0.8716758
S433	460	149.71939	6.0833333	68.266667	5.6109589	LDB	24.2	0.5730628
S434	460	159.38148	6.0833333	51.2	4.2082192	LDB	25.5	0.5576774
S435	460	168.37694	6.0833333	40.96	3.3665753	LDB	26	0.5282246
S436	460	176.76066	6.0833333	34.133333	2.8054795	LTB	27.2	0.5159566
S437	460	141.71599	4.5625	68.266667	7.4812785	LDB	33.9	0.6444923
S438	460	149.34887	4.5625	51.2	5.6109589	LDB	35.6	0.6354229
S439	460	156.53444	4.5625	40.96	4.4887671	LDB	36.9	0.6206707
S440	460	163.30157	4.5625	34.133333	3.7406393	LDB	38.2	0.6075261
S441	460	136.68677	3.65	68.266667	9.3515982	LDB	42.3	0.6717274
S442	460	142.98453	3.65	51.2	7.0136986	LDB	45.5	0.6859762
S443	460	148.96082	3.65	40.96	5.6109589	LDB	47.2	0.6773271
S444	460	154.63147	3.65	34.133333	4.6757991	LDB	50	0.6845326
S445	460	133.2275	3.0416667	68.266667	11.221918	LDB	52.9	0.7212338
S446	460	138.57622	3.0416667	51.2	8.4164384	LDB	56.8	0.7411775
S447	460	143.68279	3.0416667	40.96	6.7331507	LDB	60.7	0.7594802
S448	460	148.556	3.0416667	34.133333	5.6109589	LDB	61.4	0.73788
S449	550	149.71939	6.0833333	68.266667	5.6109589	LDB	25	0.4951331
S450	550	159.38148	6.0833333	51.2	4.2082192	LDB	25.9	0.4737375
S451	550	168.37694	6.0833333	40.96	3.3665753	LDB	27.1	0.4604789
S452	550	176.76066	6.0833333	34.133333	2.8054795	LTB	28.5	0.4521518
S453	550	141.71599	4.5625	68.266667	7.4812785	LDB	34	0.54062
S454	550	149.34887	4.5625	51.2	5.6109589	LDB	36.4	0.5433872
S455	550	156.53444	4.5625	40.96	4.4887671	LDB	37.6	0.528954
S456	550	163.30157	4.5625	34.133333	3.7406393	LDB	38.7	0.5147635
S457	550	136.68677	3.65	68.266667	9.3515982	LDB	44.7	0.593684
S458	550	142.98453	3.65	51.2	7.0136986	LDB	47.9	0.603988
S459	550	148.96082	3.65	40.96	5.6109589	LDB	49.8	0.5976968
S460	550	154.63147	3.65	34.133333	4.6757991	LDB	51.1	0.5851136
S461	550	133.2275	3.0416667	68.266667	11.221918	LDB	54.1	0.6168972
S462	550	138.57622	3.0416667	51.2	8.4164384	LDB	58	0.6329903
S463	550	143.68279	3.0416667	40.96	6.7331507	LDB	62.9	0.6582237
S464	550	148.556	3.0416667	34.133333	5.6109589	LDB	64.8	0.6513096
S465	690	149.71939	6.0833333	68.266667	5.6109589	LDB	25.7	0.4057221
S466	690	159.38148	6.0833333	51.2	4.2082192	LDB	27	0.3936546
S467	690	168.37694	6.0833333	40.96	3.3665753	LDB	28.2	0.381947
S468	690	176.76066	6.0833333	34.133333	2.8054795	LTB	29.5	0.3730568
S469	690	141.71599	4.5625	68.266667	7.4812785	LDB	35.5	0.4499405
S470	690	149.34887	4.5625	51.2	5.6109589	LDB	37	0.4402743
S471	690	156.53444	4.5625	40.96	4.4887671	LDB	37.6	0.42163

(*continued on next page*)

(*continued*)

Sample	F_y	λ	B/2t	h/s	(h/s)/(B/t)	mode	P_{FE}	P_{FE}/P_{px}
S472	690	163.30157	4.5625	34.133333	3.7406393	LDB	40.3	0.4272828
S473	690	136.68677	3.65	68.266667	9.3515982	LDB	45.8	0.4848718
S474	690	142.98453	3.65	51.2	7.0136986	LDB	49.2	0.4945059
S475	690	148.96082	3.65	40.96	5.6109589	LDB	50.8	0.4859917
S476	690	154.63147	3.65	34.133333	4.6757991	LDB	53.1	0.4846491
S477	690	133.2275	3.0416667	68.266667	11.221918	LDB	55.8	0.5071814
S478	690	138.57622	3.0416667	51.2	8.4164384	LDB	61.3	0.5332651
S479	690	143.68279	3.0416667	40.96	6.7331507	LDB	64.7	0.5396855
S480	690	148.556	3.0416667	34.133333	5.6109589	LDB	67.2	0.538388

References

[1] Husain MU, Speirs WG. Experiments on castellated steel beams. J Am Welding Soc Weld Res Suppl 1973;52(8):329–42.

[2] Kerdal D, Nethercot DA. Failure modes for castellated beams. J Constr Steel Res 1984;4(4):295–315. https://doi.org/10.1016/0143-974X(84)90004-X.

[3] Redwood R, Demirdjian S. Castellated beam web buckling in shear. J Struct Eng 1998;124(10):1202–7. https://doi.org/10.1061/(ASCE)0733-9445(1998)124:10(1202).

[4] Zaarour W, Redwood R. Web buckling in thin webbed castellated beams. J Struct Eng 1996;122(8):860–6. https://doi.org/10.1061/(ASCE)0733-9445(1996)122:8(860).

[5] Y. Sharifi J.K. Paik Maintenance and repair scheme for corroded stiffened steel box girder bridges based on ultimate strength reliability and risk assessments. Eng Struct Technol, 6 3 2014 95 105 10.3846/2029882X.2014.972991.

[6] Y. Sharifi S. Tohidi Lateral-torsional buckling capacity assessment of web opening steel girders by artificial neural networks – elastic investigation Front. Struct. Civ. Eng. 8 2 2014 167 177 10.1007/s11709-014-0236-z.

[7] Tohidi S, Sharifi Y. Inelastic lateral-torsional buckling capacity of corroded web opening steel beams using artificial neural networks. IES J Part A: Civil Struct Eng 2015;8(1):24–40. https://doi.org/10.1080/19373260.2014.955139.

[8] Sharifi Y, Hosseinpour M, Moghbeli A, Sharifi H. Lateral torsional buckling capacity assessment of castellated steel beams using artificial neural networks. Int J Steel Struct 2019;19(5):1408–20. https://doi.org/10.1007/s13296-019-00217-3.

[9] Sharifi Y, Moghbeli A, Hosseinpour M, Sharifi H. Study of neural network models for the ultimate capacities of cellular steel beams. Iran J Sci Technol Trans Civ Eng 2020;44(2):579–89. https://doi.org/10.1007/s40996-019-00281-z.

[10] Sharifi Y, Moghbeli A, Hosseinpour M, Sharifi H. Neural networks for lateral torsional buckling strength assessment of cellular steel I-beams. Adv Struct Eng 2019;22(9):2192–202. https://doi.org/10.1177/1369433219836176.

[11] Paik JK. Ultimate limit state analysis and design of plated structures. Second Edition. Chichester, UK: John Wiley & Sons; 2018.

[12] Tohidi S, Sharifi Y. Neural networks for inelastic distortional buckling capacity assessment of steel I-beams. Thin-Walled Struct 2015;94:359–71. https://doi.org/10.1016/j.tws.2015.04.023.

[13] Tohidi S, Sharifi Y. Restrained distortional buckling capacity of half-through bridge girders. IES J Part A: Civil Struct Eng 2014;7(3):163–73. https://doi.org/10.1080/19373260.2014.921400.

[14] Tohidi S, Sharifi Y. A new predictive model for restrained distortional buckling strength of half-through bridge girders using artificial neural network. KSCE J Civ Eng 2014;10(3):325–50.

[15] Tohidi S, Sharifi Y. Empirical modeling of distortional buckling strength of half-through bridge girders via stepwise regression method. Adv Struct Eng 2015;18(9):1383–97. https://doi.org/10.1260/1369-4332.18.9.1383.

[16] Bradford MA. Lateral-distortional buckling of steel I – Section members. J Constr Steel Res 1992;23(1-3):97–116. https://doi.org/10.1016/0143-974X(92)90038-G.

[17] Bradford MA. Buckling of elastically restrained beams with web distortions. Thin-Walled Struct 1988;6(4):287–304. https://doi.org/10.1016/0263-8231(88)90005-5.

[18] Bradford MA, Trahair NS. Distortional buckling of I-beams. J Struct Div ASCE 1981;107(2):355–70.

[19] Bradford MA. Distortional buckling of elastically restrained cantilevers. J Constr Steel Res 1998;47(1-2):3–18. https://doi.org/10.1016/S0143-974X(98)80003-5.

[20] Bradford MA, Wee A. Analysis of buckling tests on beams on seat supports. J Constr Steel Res 1994;28(3):227–42. https://doi.org/10.1016/0143-974X(94)90065-5.

[21] Vrcelj Z, Bradford MA. Elastic distortional buckling of continuously restrained I-section beam–columns. J Constr Steel Res 2006;62(3):223–30. https://doi.org/10.1016/j.jcsr.2005.07.014.

[22] Zirakian T. Elastic distortional buckling of doubly symmetric I-shaped flexural members with slender webs. J Constr Steel Res 2008;46:466–75.

[23] Zirakian T, Showkati H. Distortional buckling of castellated beams. J Constr Steel Res 2006;62(9):863–71. https://doi.org/10.1016/j.jcsr.2006.01.004.

[24] ABAQUS standard user's manual. Hibbitt, Karlsson and Sorensen, Inc. vols. 1, 2 and 3. Version 6.8-1. USA. 2008.

[25] Ellobody E. Nonlinear analysis of cellular steel beams under combined buckling modes. Thin-Walled Structures 2012;52:66–79. https://doi.org/10.1016/j.tws.2011.12.009.

[26] Eurocode 3. Design of Steel Structures Part 1–1: General Rules and Rules for Buildings, European Committee for Standardization (ECS). Brussels: Belgium; 2005.

[27] Schafer BW, Peköz T. Computational modeling of cold-formed steel: characterizing geometric imperfections and residual stresses. J Constr Steel Res 1998;47(3):193–210. https://doi.org/10.1016/S0143-974X(98)00007-8.

[28] Soltani MR, Bouchaïr A, Mimoune M. Nonlinear FE analysis of the ultimate behavior of steel castellated beams. J Constr Steel Res 2012;70:101–14. https://doi.org/10.1016/j.jcsr.2011.10.016.

[29] El-Sawy KM, Sweedan AMI, Martini MI. Moment gradient factor of cellular steel beams under inelastic flexure. J Constr Steel Res 2014;98:20–34. https://doi.org/10.1016/j.jcsr.2014.02.007.

[30] Sonck D, Belis J. Lateral–torsional buckling resistance of cellular beams. J Constr Steel Res 2015;105:119–28. https://doi.org/10.1016/j.jcsr.2014.11.003.

[31] Ellobody E. Interaction of buckling modes in castellated steel beams. J Constr Steel Res 2011;67(5):814–25. https://doi.org/10.1016/j.jcsr.2010.12.012.

[32] Young B, Ellobody E. Buckling analysis of cold-formed steel lipped angle columns. J Struct Eng 2005;131(10):1570–9. https://doi.org/10.1061/(ASCE)0733-9445(2005)131:10(1570).

[33] Chen S, Jia Y. Numerical investigation of inelastic buckling of steel–concrete composite beams prestressed with external tendons. Thin-Walled Struct 2010;48(3):233–42. https://doi.org/10.1016/j.tws.2009.10.009.

[34] Gholizadeh S, Pirmoz A, Attarnejad R. Assessment of load carrying capacity of castellated steel beams by neural networks. J Constr Steel Res 2011;67(5):770–9. https://doi.org/10.1016/j.jcsr.2011.01.001.

[35] Mohebkhah A. The moment-gradient factor in lateral–torsional buckling on inelastic castellated beams. J Constr Steel Res 2004;60(10):1481–94. https://doi.org/10.1016/j.jcsr.2004.02.002.

[36] Mohebkhah A. Lateral buckling resistance of inelastic I-beams under off-shear center loading. Thin-Walled Struct 2011;49(3):431–6. https://doi.org/10.1016/j.tws.2010.11.007.

[37] Australian Standards AS4100. Steel structures. Sydney (Australia): Standards Australia, AS4100-1998; 1998.

[38] AISC. Specification for structural steel buildings. American institute for steel construction. Reston (Chicago, Illinois, USA): ANSI/AISC 360-05; 2005.